CNRS
Centre National de la Recherche Scientifique

INFN
Istituto Nazionale di Fisica Nucleare

The consequences of using the etalon effect to tune the arm cavity finesse on the alignment signals for Advanced Virgo

VIR-027A-08

M. Mantovani, A. Freise, S. Hild

Issue: 1

Date: April 28, 2008

VIRGO * A joint CNRS-INFN Project
Via E. Amaldi, I-56021 S. Stefano a Macerata - Cascina (Pisa)
Secretariat: Telephone (39) 050 752 521 * FAX (39) 050 752 550 * Email W3@virgo.infn.it

Contents

1 Introduction **2**

2 Modeling the spherical/spherical cavity **2**

3 Alignment signal optical gain dependence on the etalon tuning **3**

4 Effect of the misalignment between the front and back face of the terminal mirror **4**
4.1 Amplitude of the TEM_{10} mode of the carrier as a function of the misalignment of the terminal mirror back face 5

5 Conclusions **6**

A Longitudinal locking scheme **6**

B Alignment control of the terminal mirror **7**

1 Introduction

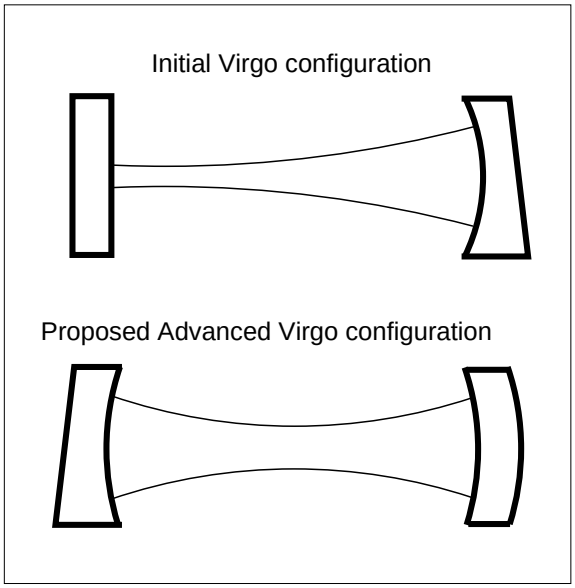

Figure 1: Comparison between the arm cavity configuration for initial Virgo (upper drawing), and the Advanced Virgo configuration as proposed by the authors (bottom drawing). In the initial Virgo optical lay-out the arms are constituted by plano-concave cavities in which the beam waist is located at the input mirror. In this case the etalon effect is driven by the flat/flat input mirror. In the Advanced Virgo optical lay-out the beam waist is located at the center of the cavity to reduce the thermal noise contribution from the input mirror. Since in this configuration the input a mirror will feature a wedge, in order to detect the cavity pick-off beam, the etalon effect could be driven by a curved/curved terminal mirror.

The main differences between the optical configuration of the initial Virgo and the Advanced Virgo will be the presence of the signal recycling mirror and the spherical/spherical long arm cavities [1]. The replacement of the plano/concave cavities present in initial Virgo has been done in order to reduce the thermal noise on the input mirrors. In initial Virgo, the etalon effect, which permits to tune the cavity finesse by varying the cavity losses, is driven by the flat/flat input mirror, see Figure 1.
The design of Advanced Virgo takes the possibility into account to have pick-off beams at the input mirrors, implying wedged input mirrors, which will strongly reduce the tuning range of the etalon effect. One possibility will be then to drive it by using the terminal mirror which can be constituted by curved/curved faces, having identical radius of curvature, such as it is shown in Figure 1.

2 Modeling the spherical/spherical cavity

parameter	length [m]
cavity length	2999.9
IMX R_c 1th face	flat
IMX R_c 2th face	1910
EMX R_c 1th face	1910
EMX R_c 2th face	1910

Table 1: Optical parameters of the simulated single cavity.

Since both, the tuning of the etalon and also potential imperfections of the mirror structure could affect the alignment signals, these effects need to be evaluated. Therefore we performed numerical simulations, using the

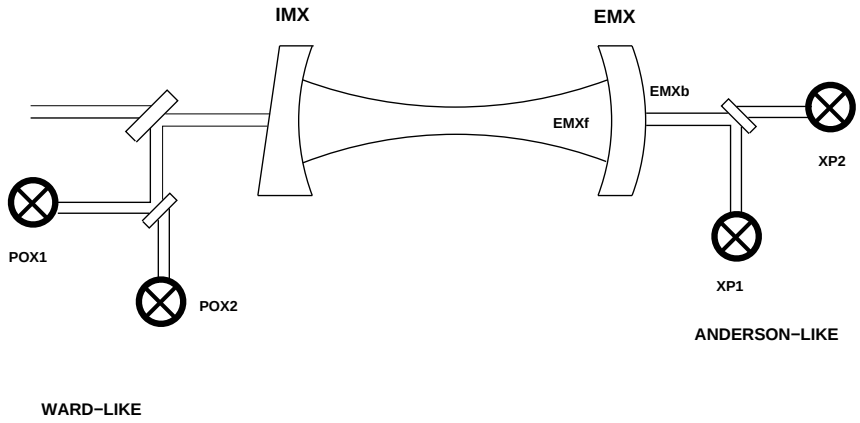

Figure 2: Schematic drawing of the cavity in which the etalon effect is driven by the end mirror. A pair of quadrant diodes is placed each in reflection and in transmission. On the input mirror (IMX) a wedge is present in order to allow the extraction of the cavity pick-off beam (POX).

frequency domain simulation *Finesse* [2]. The schematic of the simplified layout that was used for the simulation of a single arm cavity is shown in Figure 2.

The parameters used for the cavity simulation are derived from the initial parameters for the optical setup of Advanced Virgo, see Table 1. The quadrant diodes for the alignment control have been placed in reflection (POX) following the requirements for a Ward-like technique (such that no sidebands are resonant in the cavity [3]), and in transmission of the cavity (XP) as the Anderson-like technique prescribes [4] [5] (having the first higher transverse mode of the upper sideband to be resonant in the cavity). The double use of the two error signal detection techniques permits to have the possibility for an independent check.

3 Alignment signal optical gain dependence on the etalon tuning

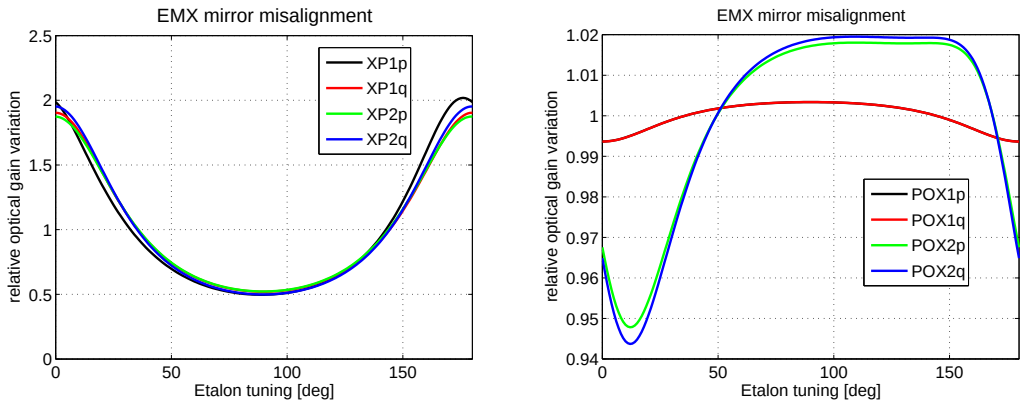

Figure 3: The optical gain as a function of the etalon tuning for the end mirror alignment signals (EMX); the left plot shows the signals detected in transmission and the right plot the signals in reflection.

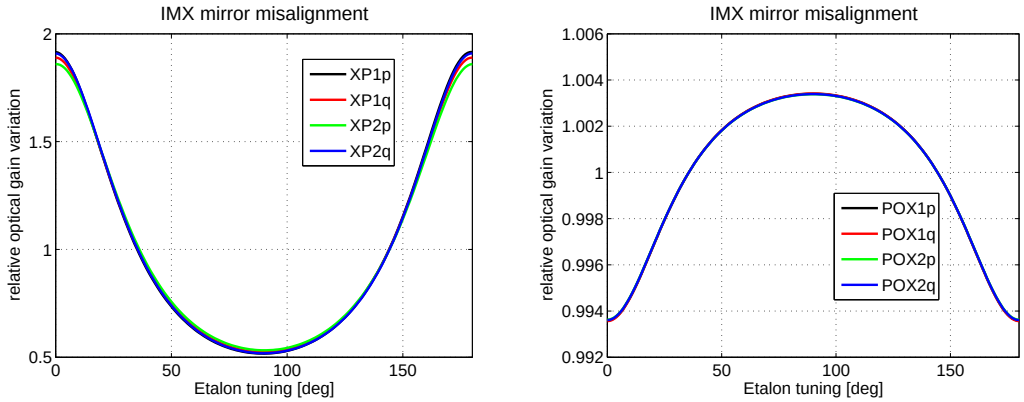

Figure 4: Optical gain as a function of the etalon effect for the input mirror alignment signals (IMX); the left plot shows the signals detected in transmission and the right plot the signals in reflection.

First of all is it interesting to evaluate how much the tuning of the etalon will affect the alignment error signals, for example to determine how much the alignment optical gain can vary as a function of the etalon effect [1]. In order to reproduce the etalon effect, the back face position of the terminal mirror (EMXb) has been tuned from 0 to 180 deg. The optical gain (g), which represents the slope of the error signal at the zero-crossing, has been computed by misaligning the mirrors in the linear region for the error signals ($\sim$ 1 nrad) in both degrees of freedom (the angular misalignment of the input and end mirrors), for each step of the etalon tuning.
Moreover, in order to have a more visible and comparable behavior of the optical gain, a relative optical gain variation (o.g.v.) has been computed as a function of the optical gain (g) as:

$$o.g.v. = \frac{g}{< g >} \tag{1}$$

As one can see from Figure 3 and Figure 4, the effect of the etalon tuning on the optical gain is especially strong (up to a factor of two) on the signal detected in transmission to the cavity (XP detection port). On the diodes placed in reflection POX detection port) the variation is much smaller ($\sim 5\%$) but still considerable.

4 Effect of the misalignment between the front and back face of the terminal mirror

Up to now the front and back faces of the terminal mirror have been considered to be perfectly parallel. In order to understand how much a misalignment between the two faces affects the alignment control signals of the interferometer, the corresponding error signals (derived from the quadrant diodes) have been simulated as a function of the misalignment between the two faces. The front surface has been considered aligned, while the back face has been misaligned. The relative misalignment will be called α.
From the results, shown in Figure 5, and considering the calibration between the quadrant signal and the front face angular displacement, we can deduce that in the linear region of the error signals, the quadrant will detect a correspondent EMX front face misalignment of $\sim 6 \cdot 10^{-5} \cdot \alpha$ rad, which is very small if we consider that the manufacture accuracy for a flat-flat mirror can give a mismatch angle better than ~ 1 μrad [6][2]. This value has

[1] In order to be confident that the longitudinal d.o.f. will not affect the alignment error signals the mirrors have been longitudinally controlled (along the optical axis) during all simulations in order to maintain the cavity at the resonance condition. This was done by using a longitudinal locking procedure which controls the cavity length by acting on the longitudinal position of the input mirror (IMX). See Appendix A.

[2] In this assumption we are considering that the performances on the manufacture accuracy of a flat-flat mirror will not be strongly different with respect to the ones which can be achieved for a curved-curved mirror. This fact is not demonstrated and it is even not trivial but it has been assumed to have an order of magnitude evaluation of the effects on the alignment signals.

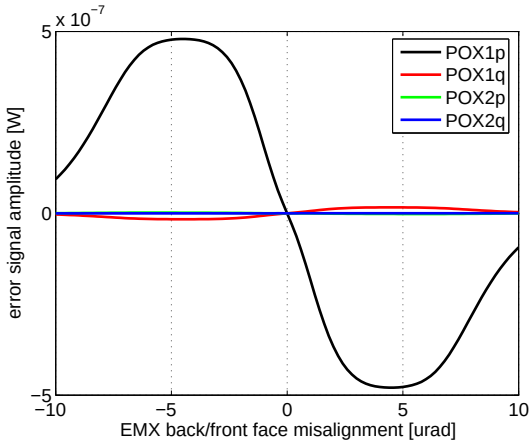

Figure 5: alignment error signal for a relative misalignment of the front face aligned and the back face misaligned. The back surface influences to some extent the alignment signals, however, the influence is very small.

been obtained by computing the ratio between the alignment error signal slope in the case of the two mirror faces had been relatively misaligned. (The alignment error signal optical gain is correct only in the error signal linear region.)
Even if the coupling between the mismatch of the faces alignment and the correspondent error signal amplitude is very weak, it is useful to understand whether the etalon causes the alignment of the cavity to fail by evaluating the amount of higher order transverse modes generated by the mismatch.

4.1 Amplitude of the TEM_{10} mode of the carrier as a function of the misalignment of the terminal mirror back face

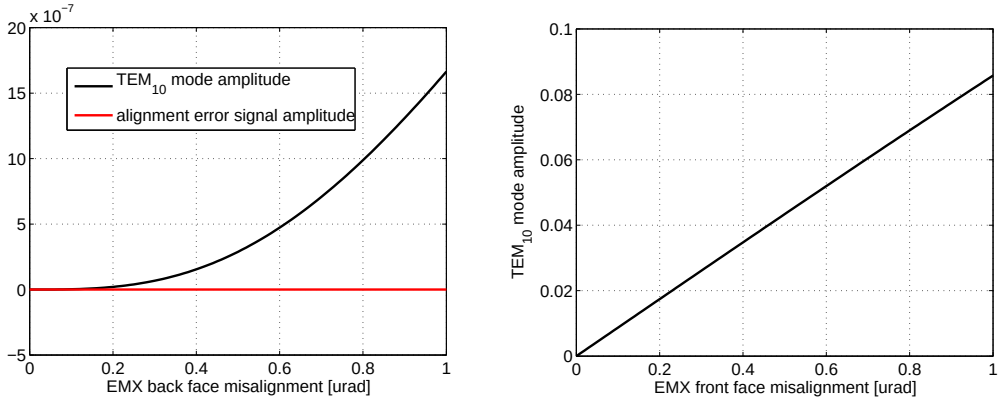

Figure 6: These plots show the amplitude of the TEM_{10} mode circulating in the cavity for two cases: on the left hand plot the back face of the etalon is misaligned while the longitudinal and the alignment feedback loops are switched on (controlling the alignment of the terminal mirror front face). The right hand plot shows for comparison the amount of TEM_{10} for a misaligned end mirror that does not feature an etalon.

If the etalon distorts in any way the alignment signal so that the feedback loop does not work properly, we would expect to have a significant amount of TEM_{10} appearing in the circulating light. Thus in order to test the propagation of the mismatch noise in the alignment signal, which is due to the difference of the alignment angle of the terminal mirror faces, we have actively controlled the angular position of the terminal mirror front face

by using an active angular control scheme (see Appendix B), while a relative misalignment has been introduced by misaligning the back face.
In the left hand plot of Figure 6 the quantity of the TEM_{10} mode and the alignment error signal amplitude is shown. In this configuration the front face of the terminal mirror has been kept aligned by the angular control loop (with an accuracy of 1 nrad) and the back face has been misaligned up to 1 μrad.
If we compare this result with the amplitude of the TEM_{10} generated by the simple misalignment of the terminal mirror in a configuration where there is no etalon (shown in the right plot of Figure 6), it is possible to calibrate the effect of the misalignment of the back face of the terminal mirror. Thus we can consider that the contribution to the TEM_{10} from the back face is negligible obtaining a correspective EMX misalignment of $6 \cdot 10^{-11}$ rad for a mismatch of 1 μrad as was demonstrated in the previous section.

5 Conclusions

In this note the consequences of an etalon effect, driven by terminal mirror of the cavity, on the alignment error signals are shown. From the results of the analysis we can conclude that the stronger effect of this optical configuration is on the alignment optical gain dependence ($\sim$ 5 % in the case the Ward-like technique and $\sim$ 200 % if the Anderson-like technique is used), see section 3. This fact will not be critical but it has to be taken into account in the control architecture design. Moreover the effect of a possible mismatch between the alignment of the back and front face will not influence strongly the alignment error signals (see section 4) which only introduces a very small quantity of higher order transverse modes circulating in the cavity. Thus from the point of view of the alignment control system there are no evident disadvantages to drive the ideal etalon effect with a curved/curved terminal mirror.

A Longitudinal locking scheme

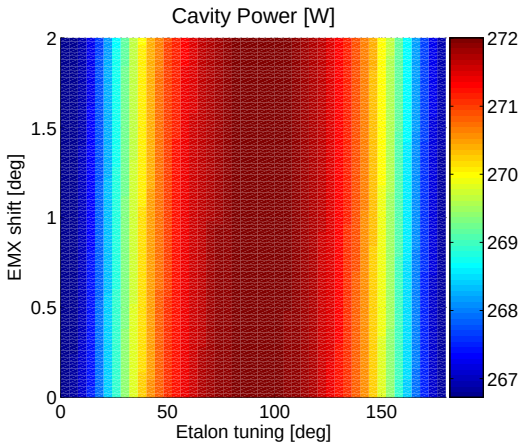

Figure 7: Cavity power behaviour as a function of the etalon tuning (from 0 to 180 deg) and of the longitudinal position of the end mirror front face (from 0 to 2 deg). It can be noticed that the longitudinal loop is well functioning allowing to reach the maximum possible power stored in the cavity, which correctly varies due to the etalon tuning (cavity finesse variation).

In order to be confident that the longitudinal d.o.f. will not affect the alignment error signals the mirrors have been placed at the correct longitudinal working point by using a continuous longitudinal locking procedure with an accuracy of 0.1 nm. The cavity has been locked by using the POX longitudinal diode demodulated at the

Anderson modulation frequency [3] and the corrections have been applied to the input mirror. In the Figure 7 one can see that the longitudinal locking is correctly functioning and the cavity power changes only due the effect of the etalon tuning which varies the finesse of the cavity.

B Alignment control of the terminal mirror

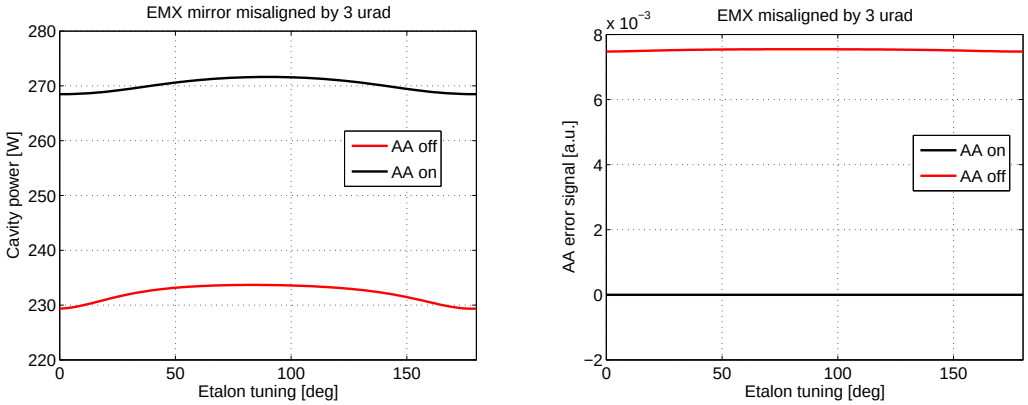

Figure 8: On the left plot the cavity power has been simulated with an alignment control loop on and off for a EMX misalignment of 3 μrad. We can see that the power, when the alignment control is engaged, corresponds to the correct value. On the right hand plot the alignment error signals for the two configurations are shown. It is kept correctly to zero when the loop is engaged.

To properly quantify the influence of a possible mismatch between the alignment of the front and back face of the mirror which should be used to drive the etalon effect (EMX) we have to be sure that the front face is properly aligned in such a way to assure that the detected effect of the back/front face misalignment will be, within an accuracy of better than 1 nrad. The angular position of the front face of the terminal mirror has been actively controlled, besides the longitudinal control, by using the signal coming from the quadrant diodes placed in reflection and feeding back to the end mirror front face (Ward-like technique). The loop gain has been computed by scanning the misalignment angle of the terminal mirror, maintaining the front and back faces of the mirror aligned between themselves.
The functioning of the control loop of the alignment can be easily demonstrated by slightly misaligning the terminal mirror and comparing the behavior of the cavity power and its error signals in the cases in which the alignment loop has been activated or not. When the loop is activated the error signal is zero and the optical power behaves as expected, see Figure 8.

References

[1] M. Mantovani, A. Freise, "Initial set of optical parameters for numerical simulations towards Advanced Virgo" Virgo note VIR-002B-07

[2] A. Freise, G. Heinzel, H. Lück, R. Schilling, B. Willke and K. Danzmann, "Frequency domain interferometer simulation with higher-order spatial modes", Class. Quant. Grav. **21** (2004) S1067 [arXiv:gr-qc/0309012].

[3] E. Morrison, *Appl. Opt.* **33** (1994), 5041 .

[3]The locking scheme has not been designed in order to have a optimum locking scheme but only to ensure that the longitudinal position of the mirrors is controlled in order to keep the cavity on resonance.

[4] D. Babusci, H. Fang, G. Giordano, G. Matone, L. Matone, V. Sannibale, "Alignment procedure for the VIRGO interferometer: experimental results from the Frascati prototype", *Phys. Lett. A* **226**, 31–40 (1997).

[5] D. Z. Anderson, "Alignment of resonant optical cavities", *Appl. Opt.* **23** (1984) 2944-2949 . 2

[6] "Virgo Input mirror substrates characterization", VIR-SPE-LYO-4340-012. 3